Y. Wittwer, R. Eichler*, D. Herrmann, and A. Türler

Supporting Information

https://doi.org/XXX, Received ...; accepted ...

Keywords: Transition metals, carbonyl complexes, single atom chemistry

PACS: ...

Communicated by: ...

S1 Ion-range simulations

To investigate the impact of kinetic energy, the thermalization of fission products in the reaction chamber of FORA was simulated. The simulations consisted of three steps. In a first step, the initial trajectory of fission products entering the reaction chamber was determined. In the second step, the data from step one were used to calculate the ranges of fission products in various media including scattering. Finally, in the third step, the real position of nuclei after stopping in the reaction chamber was estimated by combining the previous two data sets.

S1.1 Determination of fission product trajectories

After spontaneous fission of a ^{252}Cf-nucleus, the generated fission products are recoiling in a 180-degree angle away from each other with high kinetic energy. With a certain probability, one of the two fission products will be able to pass through the hole in the aluminum-wheel separating the ^{252}Cf-source from the reaction chamber as depicted in figure S1.

Y. Wittwer, R. Eichler, D. Herrmann, Paul Scherrer Institute, Switzerland
Y. Wittwer, A. Türler, University of Bern, Switzerland

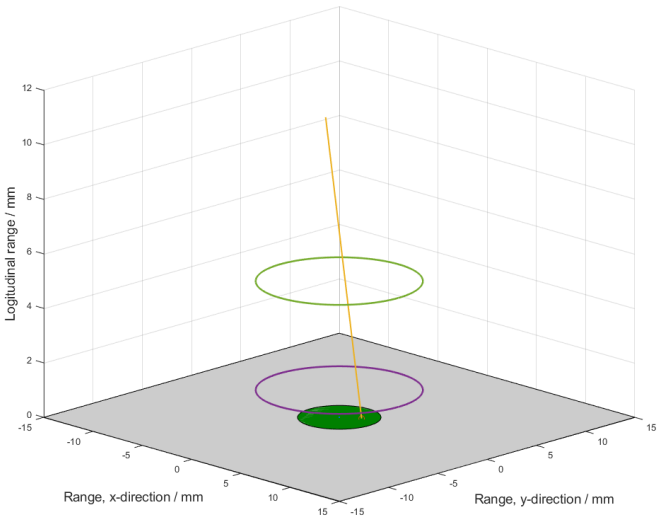

Fig. S1: Illustration of the Monte Carlo simulations performed showing a single trajectory. The green surface corresponds to the ^{252}Cf-source. The purple and green circle correspond to the entrance and outlet of the collimator hole in the aluminum-wheel between source and reaction chamber. The origin of the coordinate system shown corresponds to the middle of the ^{252}Cf-source.

The hole in the aluminum-wheel serves as a collimator to allow only fission products with specific trajectories to pass through. The process of fission products entering the reaction chamber was simulated using a custom made Monte Carlo simulation written in Matlab. The ^{252}Cf-source has a diameter of 6 mm with a circular shape. The entire source is covered with a 6 μm thick aluminum-foil to avoid contamination of the system with ^{252}Cf itself. Since part of this foil was damaged in the past, about 1/3 of the source was covered with an additional, thick aluminum-foil which is not penetrable by fission products. This was taken into account for the purpose of simulations. The workflow of the simulation can be described as follows:

1. In a first step, a random position is determined on the surface of a circle with a diameter of 14 mm. This corresponds to a spontaneous fission decay of a ^{252}Cf-nucleus on the source assuming the Cf-atoms to be homogeneously distributed on the Pt-carrier. If the random position corresponds to a sealed part of the source, it is rejected.

2. For each random position, a random emission trajectory is determined by generating a polar and azimuth angle corresponding to a uniform, spherical distribution. The trajectory is assumed to be a straight line. It is checked if a particle following the previously determined trajectory is able to pass the hole in the aluminum-wheel, the collimator, and enters thereby the reaction chamber. This is done by checking if the particle is able to pass through the surface of two circles with a diameter of 12 mm each, being 4 mm away from each other. This corresponds to the geometry of the wheel-collimator.
3. If the particle penetrates the two holes, i.e., it goes through the two circles, it is accepted. The trajectory corresponds to a possible entrance path into the reaction chamber. The two emission angles and the starting position of the particle on the ^{252}Cf-source are stored.

The workflow illustrated above was repeated until 10'000 trajectories corresponding to particles entering the reaction chamber were collected. Physically, this corresponds to the situation in a vacuum.

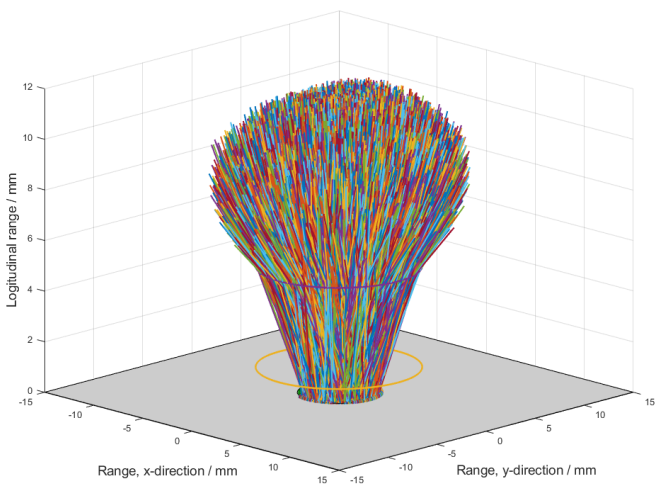

Fig. S2: Simulation performed for 10'000 particle trajectories being able to enter the reaction chamber through the collimator. Compare with figure S1, where only one trajectory is shown.

S1.2 Ranges and scattering

To simulate the influence of the process gas and degrader foils on recoiling fission products, the previously described Monte Carlo simulations were combined with the SRIM software [1]. SRIM allows the user to define a batch file containing energies and emission angles for different nuclei. After defining the target in which the particles shall be emitted, the SRIM software calculates the position of each pre-defined nucleus in the target after stopping in x,y,z-coordinates. This includes scattering effects of nuclei. The 10'000 trajectories obtained above were written into a batch file suitable to be read by the SRIM software. The targets were chosen to resemble the experimentally investigated systems. A summary of the defined targets including densities and compound correction factors is given in table S3. After obtaining the position of nuclei in the target by SRIM, it is important to note that SRIM does take into account different emission angles, but not different starting positions. Therefore, the SRIM simulations correspond to the stopping of nuclei assuming they were all emitted from the middle of the ^{252}Cf-source. In order to estimate the real position of emitted nuclei, the emission point of the fission product on the source surface has to be taken into account. It is simply added to the x and y end coordinates:

$$\begin{bmatrix} x_{eff} \\ y_{eff} \\ z_{SRIM} \end{bmatrix} = \begin{bmatrix} x_{source} \\ y_{source} \\ 0 \end{bmatrix} + 1.4 * \begin{bmatrix} x_{SRIM} \\ y_{SRIM} \\ z_{SRIM} \end{bmatrix} \quad (1)$$

where x_{eff}, y_{eff} and z_{SRIM} are the final coordinates of the injected nuclei after being stopped in the chamber. x_{source} and y_{source} correspond to the emission point on the ^{252}Cf-source for a specific trajectory, and x_{SRIM}, y_{SRIM} and z_{SRIM} are the stopping coordinates as given by the SRIM software for a nuclei ejected with the former trajectory. The factor of 1.4 is a correction factor determined by D. Wittwer, that accounts for the underestimation of ion ranges in the gas-phase by the SRIM program [2].

In conclusion, for each combination of starting point on the source and emission angle, three coordinates are obtained corresponding to the point in the reaction chamber, where the corresponding particle is thermalized. This was simulated for 10'000 particles under all experimental conditions. Simulations were done for ^{104}Mo with an initial energy of 103 MeV [3].

The simulations indicate an increased density of particles being stopped slightly

above the degrader foil. This actually corresponds to particles being stopped in the degrader foil prior to entering the reaction chamber. The reason those particles appear to be stopped above the position of the actual degrader foil is the correction factor applied to account for the underestimation of stopping powers by SRIM in the gas-phase (cf. equation 1). While leading to a more realistic distribution of particles being stopped in the reaction chamber, the correction factor causes an overestimation of ranges for ions being stopped in the degrader foil. However, particles being stopped in the degrader foil are not considered to be relevant for the formation of MCCs. Since the fission source is covered by an additional, 6 μm thick foil to avoid contamination of the system with ^{252}Cf itself, particles having flat emission angles are stopped early and do therefore not enter the reaction chamber.

S2 Overall transport

The overall transport time and resulting decay during transport was estimated using a simple approach based on volume and gas flow.

$$t = \frac{V}{Q_{real}} \tag{2}$$

t is the estimated transport time for an MCC to reach the charcoal trap, Q_{real} is the actual gas flow and V is assumed as 75% of the volume of the reaction chamber, to account for the range of fission products, plus the volume of the pipes connecting the chamber to the charcoal trap. From this, the decay during transport is calculated using:

$$N_i(t) = N_{i,0} * e^{-\lambda_i * t} \tag{3}$$

with N_i(t) being the number of atoms from isotope i reaching the charcoal trap and λ_i being the decay constant of isotope i. $N_{i,0}$ was arbitrarily set to 10000 to calculate the fraction of atoms reaching the charcoal trap for each isotope.

S3 Input-values

S3.1 Adsorption input

For the adsorption simulations, the input values in table S1 and S2 were used.

Tab. S1: Constant input parameters used for the adsorption simulations. The density of the adsorbate (MCC) was assumed to be 1.96 g/ml for all MCCs. The dependency of the simulation on the adsorbate density is small, therefore this simplification is not expected to affect the overall result.

Parameter	Value
Number of simulated molecules	10'000
Chamber diameter	40 mm
Chamber length	72 mm
Column diameter	2 mm
Column length	2 m
Gas pressure	1 bar (0.987 atm)
Temperature	298.15 K
Molar mass of gas	28 g/mol
Density of gas at m.p.	0.789 g/ml
Density of adsorbate at m.p.	1.96 g/ml
Maximal lattice phonon frequency of TEFLON	3*10^{13} s^{-1}

Tab. S2: Variable input parameters used for the adsorption simulations. "m.p." stands for melting point.

Parameter	Value
Molar mass ($^{104}Mo(CO)_6$)	272 g/mol
Molar mass ($^{110}Ru(CO)_5$)	250 g/mol
Molar mass ($^{107}Tc(CO)_5$)	247 g/mol
Molar mass ($^{111}Rh(CO)_4$)	223 g/mol
Half-life (^{104}Mo)	60 s
Half-life (^{110}Ru)	12.04 s
Half-life (^{107}Tc)	21.2 s
Half-life (^{111}Rh)	11 s
Adsorption enthalpy ($^{104}Mo(CO)_6$)	-38 kJ/mol [4]
Adsorption enthalpy ($^{110}Ru(CO)_5$)	-34 kJ/mol [5]
Adsorption enthalpy ($^{107}Tc(CO)_5$)	-43 kJ/mol [6]
Adsorption enthalpy ($^{111}Rh(CO)_4$)	-36 kJ/mol [5]

S3.2 Ion-range simulations

For the Matlab based Monte Carlo simulations, 10'000 points were simulated. The setting is schematically shown in figure S3, left panel. For the SRIM simulations, the layer setting is schematically depicted on the right panel of figure S3.

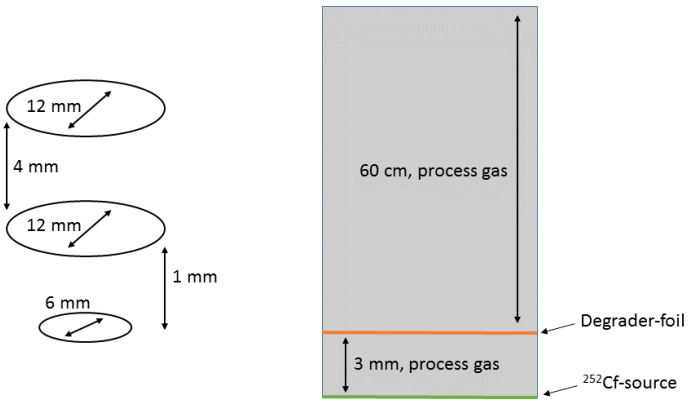

Fig. S3: Schematic representation of the geometrical setting used for the Monte Carlo (left panel) and SRIM calculations (right panel). Both setups represent the geometry in the actual FORA reaction chamber. Left panel: Shown are the three circles used to simulate the trajectory of fission products through the collimator. The circle with a diameter of 6 mm represents the ^{252}Cf-source. the two smaller circles represent the entrance and exit of the collimator wheel. Right panel: Arrangement of layers used for SRIM simulations. The locations of the ^{252}Cf-source and the degrader foil are indicated. The space between the two was defined to be process gas. After the degrader foil, 60 cm of additional process gas were defined.

The thickness of the degrader foil as well as the composition of the process gas were varied according to the investigated system. The used input values for the process gas are given in table S3. All densities and compound correction factors were calculated as the weighted sums of the properties for the individual gases.

Tab. S3: Process gas inputs used for SRIM calculations. All gases were investigated at a pressure of 1 bar. The first column represents the chemical system that was simulated, the second the gas density used. The third column corresponds to the compound correction factor (Comp. Corr.) used by SRIM to account for the effect of molecular electrons on ion stopping. The last three columns give the atomic composition of the medium, the faction of C and O atoms and in the last column the number of He/Ar/N atoms.

System	Density [g/ml]	Comp. Corr.	C-Atoms	O-Atoms	Other Atoms
100% CO	1.15 * 10^{-3}	0.811	1	1	-
50:50 CO:He	0.657 * 10^{-3}	0.906	1	1	1 He
50:50 CO:Ar	1.39 * 10^{-3}	0.906	1	1	1 Ar
50:50 CO:N_2	1.15 * 10^{-3}	0.898	1	1	2 N

S4 Partial evacuation

Since a lot of the measurements presented here require to add or/and remove process gas from the FORA-setup, a measurement series to investigate the effect of process gas manipulation on signal constancy was performed. FORA was filled with 100% CO up to 1 bar at 1000 ml/min. After operation for multiple hours (during which a gas flow study was performed), process gas was removed from the system to reduce the pressure to 0.5 bar, before fresh CO was added to stabilize the pressure again at 1.00 bar. Afterward, a series of continuous 1 hour long measurements was started. The results are shown in figure S4. A Sicapent™ and Micro Torr 602F cartridge were used for purification.

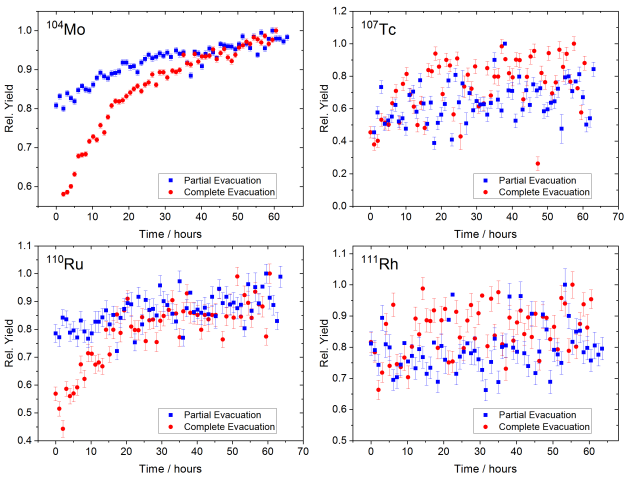

Fig. S4: Long-term measurement started after partial evacuation and refilling of FORA compared with a long-term measurement where FORA was completely evacuated and refilled before starting the measurement series. Process gas, pressure, gas flow and purification columns were identical for both measurements. The data are normalized to the highest obtained yield. The error bars correspond to the statistical counting error for each measurement.

It appears that partial evacuation of the FORA-setup does not completely reset the time-dependent change of signal previously observed. Only for ^{104}Mo, a change in signal over time is still observed after partial evacuation, if the system was already operated for some time. However, this might also just be a continuation of a trend already being present. Investigations requiring to add/remove process should be therefore suitable without strong interference of time-dependent effects, especially when considering the additional safety measures applied in this study by repetition of experiments and pseudo-randomization of the order of varied parameters during the trend measurements.

References

1. Ziegler, J. F., Ziegler, M. D., Biersack, J. P. SRIM - The Stopping and Range of Ions in Matter. Nuclear Instruments and Methods in Physics Research B 268 1818–1823 (2010).
2. Wittwer, D., Abdullin, F. S., Aksenov, N. V., Albin, Y. V., Bozhikov, G. A., Dmitriev, S. N., Dressler, R., Eichler, R., Gäggeler, H. W., Henderson, R. A., Hübener, S., Kenneally, J. M., Lebedev, V. Y., Lobanov, Y. V., Moody, K. J., Oganessian, Y. T., Petrushkin, O. V., Polyakov, A. N., Piguet, D., Rasmussen, P., Sagaidak, R. N., Serov, A., Shirokovsky, I. V., Shaughnessy, D. A., Shishkin, S. V., Sukhov, A. M., Stoyer, M. A., Stoyer, N. J., Tereshatov, E. E., Tsyganov, Y. S., Utyonkov, V. K., Vostokin, G. K., Wegrzecki, M., Wilk, P. A. Gas Phase Chemical Studies of Superheavy Elements using the Dubna Gas-Filled Recoil Separator – Stopping Range Determination. Nuclear Instruments and Methods in Physics Research B 268 28–35 (2010).
3. Schmitt, H. W., Kiker, W. E., Williams, C. W. Precision Measurements of Correlated Energies and Velocities of ^{252}Cf Fission Fragments. Physical Review 137 837–847 (1965).
4. Wang, Y., Qin, Z., Fan, F. L., Fan, F. Y., Cao, S. W., Wu, X. L., Zhang, X., Bai, J., Yin, X. J., Tian, L. L., Zhao, L., Tian, W., Li, Z., Tan, C. M., Guo, J. S., Gäggeler, H. W. Gas-Phase Chemistry of Mo, Ru, W and Os Metal Carbonyl Complexes. Radiochimica Acta 102 69–76 (2014).
5. Cao, S., Wang, Y., Qin, Z., Fan, F., Haba, H., Komori, Y., Wu, X., Tan, C., Zhang, X. Gas-Phase Chemistry of Ruthenium and Rhodium Carbonyl Complexes. Physical Chemistry Chemical Physics 18 119–125 (2016).
6. Wang, Y., Qin, Z., Fan, F. L., Haba, H., Komori, Y., Cao, S. W., Wu, X. L., Tan, C. M. Gas-Phase Chemistry of Technetium Carbonyl Complexes. Physical Chemistry Chemical Physics 17 13288–13234 (2015).